



Studying Site Effects Using Shear Wave Velocity and Microtremors in Shahrekord City

M. Mojarab¹, H. Memarian², and P. Roozkhosh³

1. MSc Student, Exploration Engineering, University of Tehran, Tehran, I.R. Iran,
email: mmojarab@gmail.com

2. Professor, School of Mining Engineering, University of Tehran, Tehran, I.R. Iran

3. Research Associate, Soil Conservation and Watershed Management Research Center,
Tehran, I.R. Iran

ABSTRACT

Here, the site effects of seismic hazard zonation of urban areas on the ground motions and earth deformations is studied in Shahrekord. The main purpose is zoning the geological engineering features and assessing the seismicity of the region. In this regard the microtremors are measured by single point sampling method and Nakamura analysis. The microtremors of all over the city are processed by J-SESAME. The information layers are prepared in GIS used for detecting the zonations of potential landslide hazard. Shear wave velocity is calculated in 20 profiles for soil classification. The microtremors are measured in 65 points and 70 wells and boreholes. To study the earth deformation, geological engineering condition is investigated using Digital Elevation Model (DEM), slope, slope orientation, soil type, soil thickness, underground water, rockfall and liquefaction maps. The natural period of site and amplification factor are analyzed using microtremor and shear-wave velocity.

Keywords:

Microtremor;
Amplification factor;
Natural period;
Shahrekord;
Landslide;
Soil classification

1. Introduction

Natural disasters, such as earthquake, flood, landslide and liquefaction are among major problems of human societies. An important intensifying factor in such disasters is the type of the site. Site effects, are divided into earth deformation and ground motion.

The first step in studying the earth deformation is to develop multi-layer engineering geology maps (e.g. slope, DEM, alluvium thickness, and sand distribution). These maps define certain factors such as landslide potential and liquefaction. In addition to earth deformation, alluvium thickness can act as a filter and change the dynamic and seismic characteristics of the signals [7]. Soil thickness first changes the frequency content and motion duration, and then causes resonance.

The earth surface is always in motion at different frequencies, even in the absence of active seismic sources. These constant vibrations are called

microseisms or preferably microtremors. The amplitude of these microtremors are generally too small (10^{-4} - 10^{-2} mm) to be felt by human senses [9]. Microtremors are considered as noise sources in seismological studies.

The amplification of the earthquake signals, recorded from distant sources, and the amplitude of microtremors increase proportionally. Therefore, the desired earthquake signals are finished in the "noises". Since the elimination of these noises is technically very difficult, they are considered as "seismic noises" or simply "noises" in earthquake studies.

Site effects can be examined by different methods, the first one is studying microtremors. Evaluation of site response by microtremor has been studied by different groups [12-20]. The most important techniques used for microtremor analysis are calculating: a) the spectral ratio of the signals received

from deposits to of those from bedrock; b) the spectral ratio of horizontal component to the vertical one. The constraint of the technique (a) is inaccessibility to the bedrock proper for station, especially in urban areas. H/V , the technique (b), without reference station, was first presented by Nogoshi and Igaroshi [7] and then developed by Nakamura [5]. The reliable results of this technique confirm its applicability in the determination of natural period and soil amplification factors.

Another method of site effect investigation is shear wave velocity classification. In fact, shear-wave velocity is used to find out the site characteristics. The site characterization (or site classification) is now based only on the properties of the first 30m of soil, including the probable rock layers. The site class is exactly determined by one parameter "average shear-wave velocity of top 30m soil", with \bar{V}_S denoted in the references. \bar{V}_S is calculated using the time that shear wave takes in traveling from 30m depth to the ground surface. The profiles of soil and rock layers have their own shear wave velocity (V_S) and thickness [10]:

$$\bar{V}_S = 30 / \left[\sum (h / v_s) \right] \quad (1)$$

The objective of \bar{V}_S calculating in this way is to classify the soil deposited on rock, even if the depth is less than 30m.

2. Geological Engineering Study

The topographic information, geological map, geometrical studies, water well excavating logs, bore

exploring, annual raining rate and aerial photos are prepared for geological aims, see Figure (1). The data are studied individually or in the combination of others. In this regard, the topographic layers are merged by 1:25000 scale and some level topographic lines are verified.

The slope, slope orientation and 3-dimensional maps of the region are prepared by topographic map. The borrow material and ground type maps are prepared using geological maps and aerial photos. They are published in another paper entitled "geological engineering zoning of Shahrekord". In order to zone the isohyets lines and prepare the relevant maps, the data of Iran Meteorological organization are used.

To study the earth deformation, the geological engineering information is prepared by different data layers. In this regard the detailed excavation data of 70 wells are used and the microtremors of 65 stations are measured.

Finally, shear-wave velocities are measured at 20 stations in Shahrekord city, see Figure (1). Shahrekord is studied for geological engineering with respect to the general development design, the available information, field visits and data combined in *ArcGIS* software. In this regard, first, the wells data are run by *ArcGIS* software and then, they are interpolated regarding the type of layers and the purpose of this research [2].

3. Thickness of Soil Layers

The data of Water Organization of Charmahal

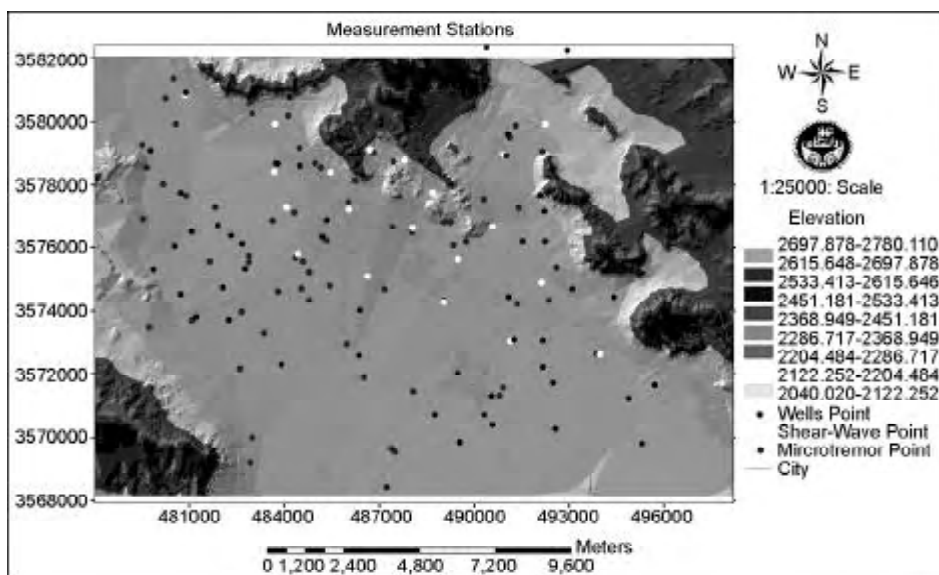


Figure 1. The station of microtremor, shear wave velocity, and geotechnical data measurement.

Bakhtiari are used to calculate the soil thickness on the bedrock. The wells are located by *UTM* coordinate after surveying the literature and gathering excavating well logs.

The soil thickness is calculated in each well concerning the excavating log and saved in *ArcGIS* software along with the wells locations. Finally, the data of zoning and soil thickness are mapped as co-level lines.

Several important points according to the alluvium thickness map, obtained in Shahrekord, are: - the maximum alluvium thickness of about 65m in the south of Kiyān city [3]; - the hollow locations of the bedrock areas, with high alluvium thickness and probably carbonated bedrocks. Besides, Shahrekord is surrounded by stoned mountains which have Karstic condition, see Figure (2).

4. Underground Water Layer

The water level is studied using the existed maps of the past years. The survey shows that the underground water level is low due to infinite drainage as well as the deviation of Kuhrang Fountain toward Isfahan.

To prepare co-level maps of water in the plain, the available water wells and pizometric data are used; and the water levels are modeled for several continuous years. The co-level maps show the decreasing of water level in approaching the present.

The underground water flow has two main branches according to Isobath underground water maps [3]; the first one, starting from northwest with a high hydraulic gradient of about 1.1% reaches the minimum of 0.14% in the south; the second is started with an

east-west slope direction and a gradient of 0.8 % and reaching the minimum of 0.3% joins the north branch in the south. The underground water level varies between 2040 and 2140m in this plain. Two zones in the west of Shahrekord have specific conditions and seem to be the containing water holes filled with alluvium in the bedrock [3]. The results of alluvium thickness study show the existence of Karst condition in these zones, see Figure (3).

5. Slope Classification and Rockfall Potential

Slope and slide of the ground are two undividable factors in ground hazard studying. The probability of landslide is nearly high in high topographic slope, regarding the slope orientation and geometrical parameters. Therefore, the slope map of the region is modeled using its topographic layers.

The processes are stepped in such a way that the 3-dimensional height map is prepared firstly in *ArcGIS* software after revising the topographic layer. Then the slope model is classified in 9 groups. The slope orientation map is obtained by slope map, see Figure (4). To provide geological hazard layers (e.g. rockfall) *DEM*, slope and Isohyetal maps are made subsequently. Slope is classified based on *DEM* map, see Figure (4). Various layers-slope, slope orientation, precipitation and acceleration are used to obtain the slide potential map [1], resulted in 3 high hazard zones-named *A*, *B* and *C*, see Figure (5). Field observations indicate that the local slides in *B* zone are rockfall. *B* zone with steep blocks is located in the north of industrial district of Shahrekord, see Figure (6).

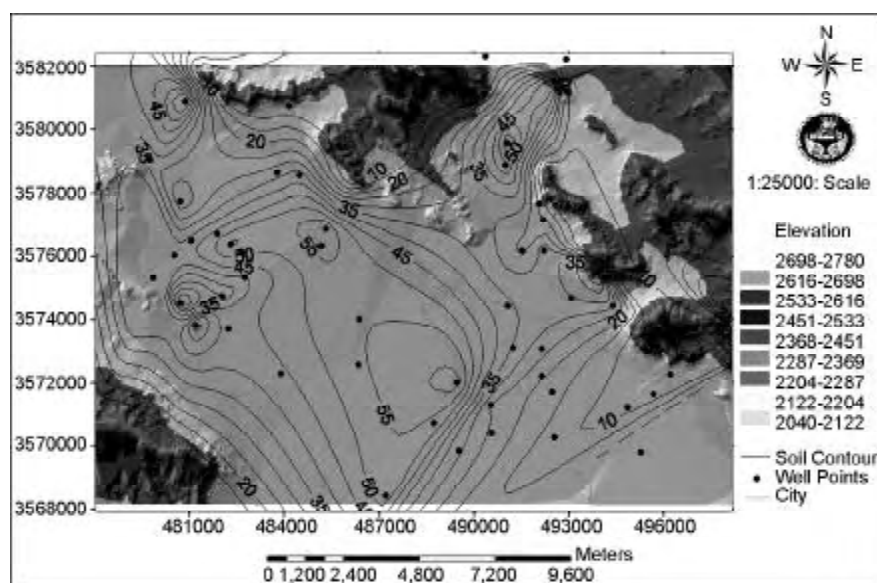


Figure 2. Soil thickness map.

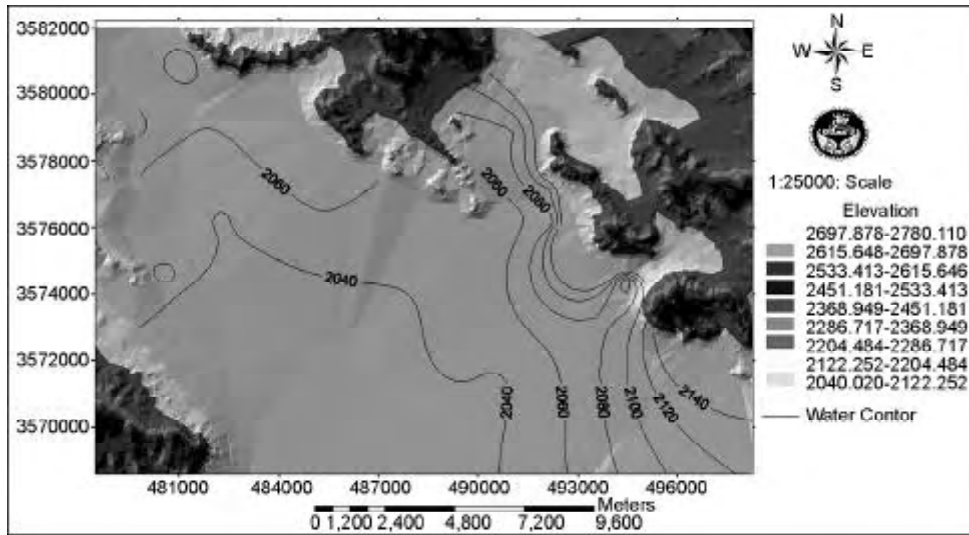


Figure 3. Underground water of Shahrekord.

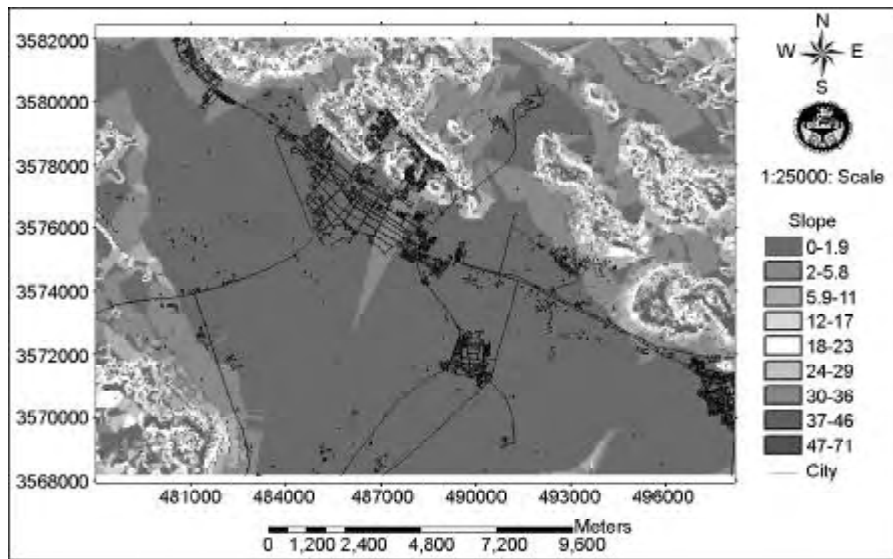


Figure 4. Slope classification of Shahrekord.

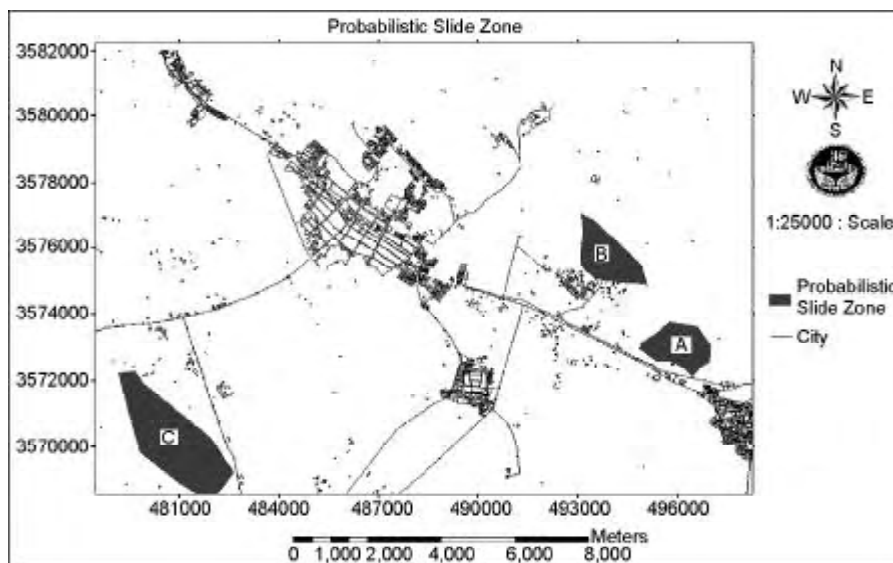


Figure 5. The zonation of rockfall potential.



Figure 6. Rockfall figures of Shahrekord industrial district.

6. Liquefaction

The most important factor in liquefactions, caused by earthquake, is the sand content saturated by water. There are only few zones containing less than 40% sand in the study area [3]. Therefore, according to the distribution map, liquefaction hazard is low because of low sand density of the surface layers and relatively low level of underground water, see Figure (7).

7. Ground Motion Investigation

H/V ratio, the Fourier spectral ratio of horizontal to vertical components of microtremors, were introduced in early 70's [5]. In the sites, located on soft soils, the spectral ratio curves show a clear peak that is in proper accordance with natural resonance period. H/V spectral ratio method, besides the

determination of site natural period, can give the amplification factor of alluvium in different stations, especially for lower frequencies [6, 11]. For recording microtremor waves, both pre-designed net stationary measurement and single portable seismometer are used. In this study, Nakamura method is used to analyze the data obtained by single-station recording. Site effects, usually considered as empirical transfer functions of the surface layers, are commonly studied by two techniques: standard spectral ratio and H/V [8]. The standard spectral ratio (S_T) is calculated by dividing the horizontal Fourier spectrum of the ground motions on an alluvium site, S_{HS} , by the one on a nearby rock site (S_{HB}), shown in Eq. (2).

$$S_T = \frac{S_{HS}}{S_{HB}} \tag{2}$$

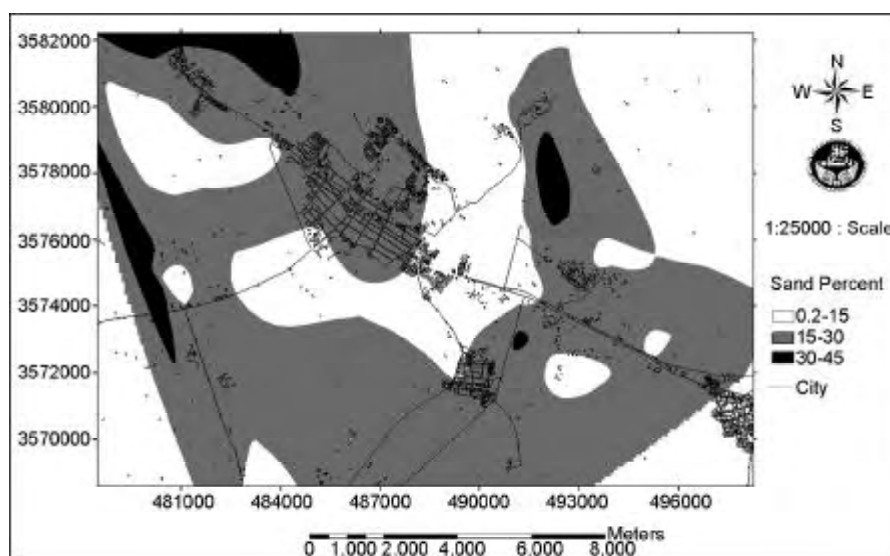


Figure 7. Sand distribution map of area.

Following Nakamura's research [5], Lermo et al [16] used spectral ratio E_S to estimate the source amplitude effect, Eq. (3).

$$E_S = \frac{S_{VS}}{S_{VB}} \quad (3)$$

where, S_{VS} and S_{VB} are Fourier spectra of the vertical motions on the ground surface and those on the bedrock at a certain depth, respectively. Nakamura [5] first assumed that the vertical component of the microtremor was not amplified by low-velocity surface layers. Then he estimated the effect of Rayleigh waves on the vertical components of the tremors by evaluating E_S [8]. He proposed that if the effects of Rayleigh waves were the same on the vertical and horizontal components, then E_S could be used to eliminate the effects of Rayleigh waves on the transfer function. In this regard, Lermo et al [16] introduced a modified site effect function (S_{TT}) to cover the source effects (E_S) in the form of Eq. (4):

$$S_{TT} = \frac{S_T}{E_S} \quad (4)$$

Which is equivalent to Eq. (5).

$$S_{TT} = \left(\frac{S_{HS}}{S_{VS}} \right) / \left(\frac{S_{HB}}{S_{VB}} \right) \quad (5)$$

Nakamura [5] also pointed out that S_{HB} to S_{VS} ratio was nearly 1 which was obtained by measuring microtremor in a borehole. Recently, Huang and Teng [21] examined the ratio using microtremors and earthquake recordings at a bedrock site in Chiawan, Taiwan. Regarding these empirical controls, here, a reasonable estimation of the modified site effect function is determined by Eq. (6):

$$S_{TT} = \frac{S_{HS}}{S_{VS}} \quad (6)$$

This suggests that H/V ratio can be obtained by the motions on the surface and make the estimation of ground motion characteristics easier. The natural frequency (NF) and the amplification factor (AP) of the site are determined by H/V ratio [6].

8. Measurement and Analysis of Microtremor

The seismometer features are:

- 24 bit seismometers (made in Italy)
- 3 Geospace geophones (made in USA)
- Steady frequency responses, between 0.2 and 50Hz

- Natural period of 1Hz.

Each record lasts 5 to 10 minutes at every station with the rate of 100 samples per second and the data are processed by *J-SESAME* software. Signal bars are divided into 10-second windows, see Figure (8). A 0.5 to 25HZ bandpass filter is used to exclude the urban noises of frequencies over 25HZ [2]. Spectral amplitude of each window is computed for Z , N , and E components using a fast Fourier transform and dividing the horizontal component average spectra by vertical one, H/V . All these steps are performed for each window. Selecting the best part for Fourier spectrum is very important in data interpreting, i.e. it should be considered both in sampling and interpreting of data. Therefore, the records should be chosen at the least level of noise or calm period of time for confronting the noises such as wind or rain. An isolated media should be considered for seismometer velocity system.

For random noises happened at the sampling area (e.g. passing cars), the times and distances from seismometer should be noted and eliminated during interpreting and selecting the proper window for calculating the Fourier spectrum. The mentioned points are considered here and used in the data interpreting, the guidelines of experienced *J-SESAME* research group. To select the proper records, the power spectra calculating method is used. The records of high power are selected for further analysis. In this project several records are registered at calm time of the day (at 1-2 in the morning) in different part of the city and are considered as the basis of selecting other records. In other words a distributed network is considered for basic points recording. The microtremors are calculated in these points repeatedly and power spectra are obtained by records, see Figure (9). In this way the decision base is gained concerning signal strength in the city. After going through the mentioned processes for all stations, the site natural period is determined by Nakamura method. Natural period is the period with maximum amplitude in H/V . Amplification factor is the length of the highest peak in H/V spectrum, shown in Figure (10) [2]. Finally, the results are presented in the form of natural period zoning and amplification m factor maps, both applicable for engineering purposes, Figure (11) and Table (1).

Natural period is classified into 9 levels with the minimum of 0.1sec. and maximum of 1.2sec. Natural periods increase as they get closer to the plain and decrease when become closer to the mountains.

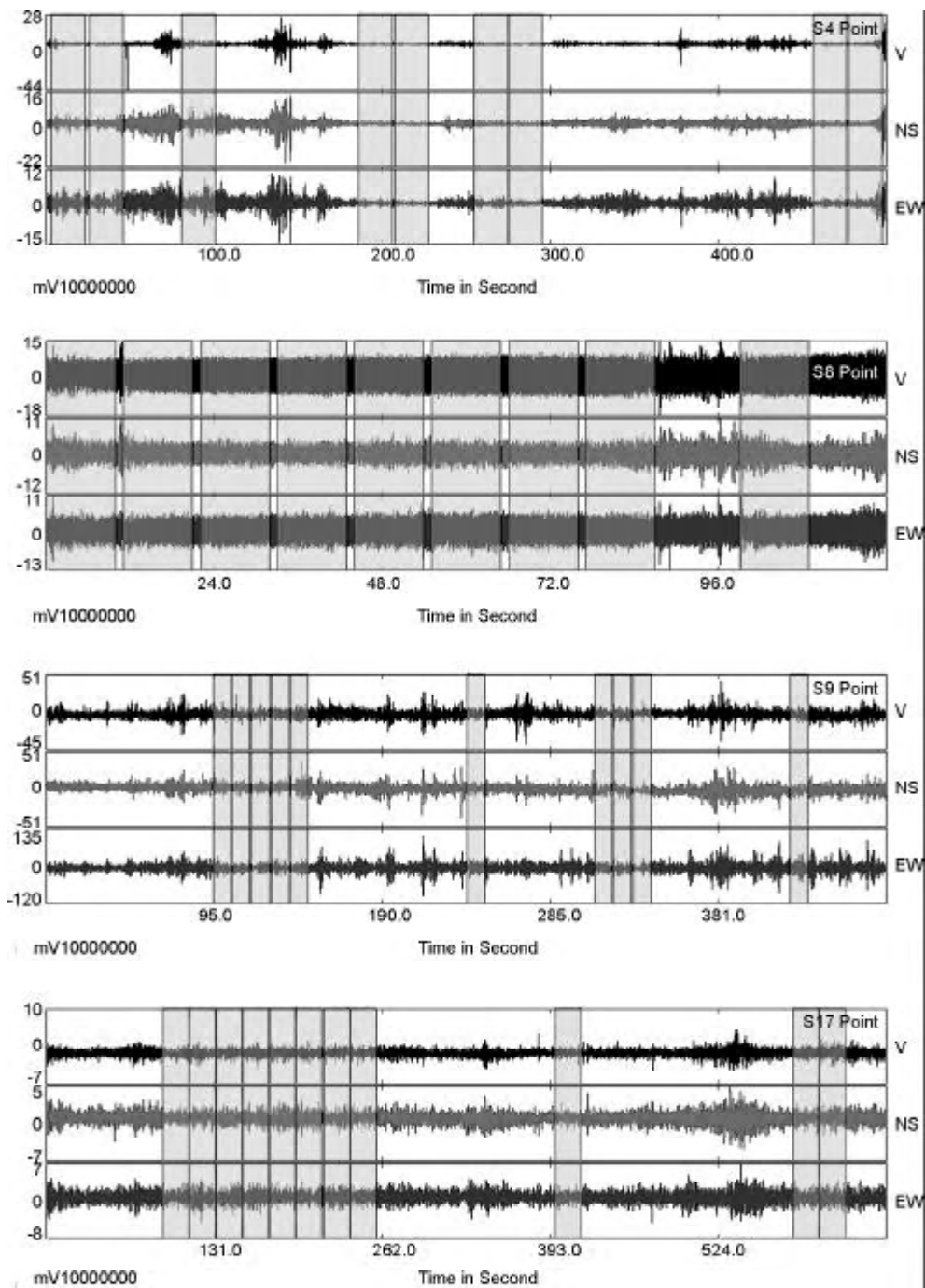


Figure 8. Microtremor measurement windows.

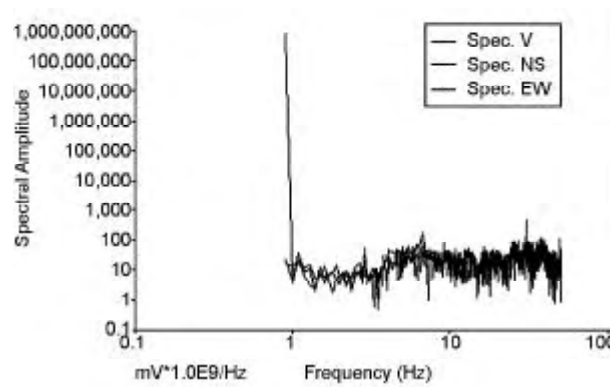


Figure 9. An example of microtremor power spectrum.

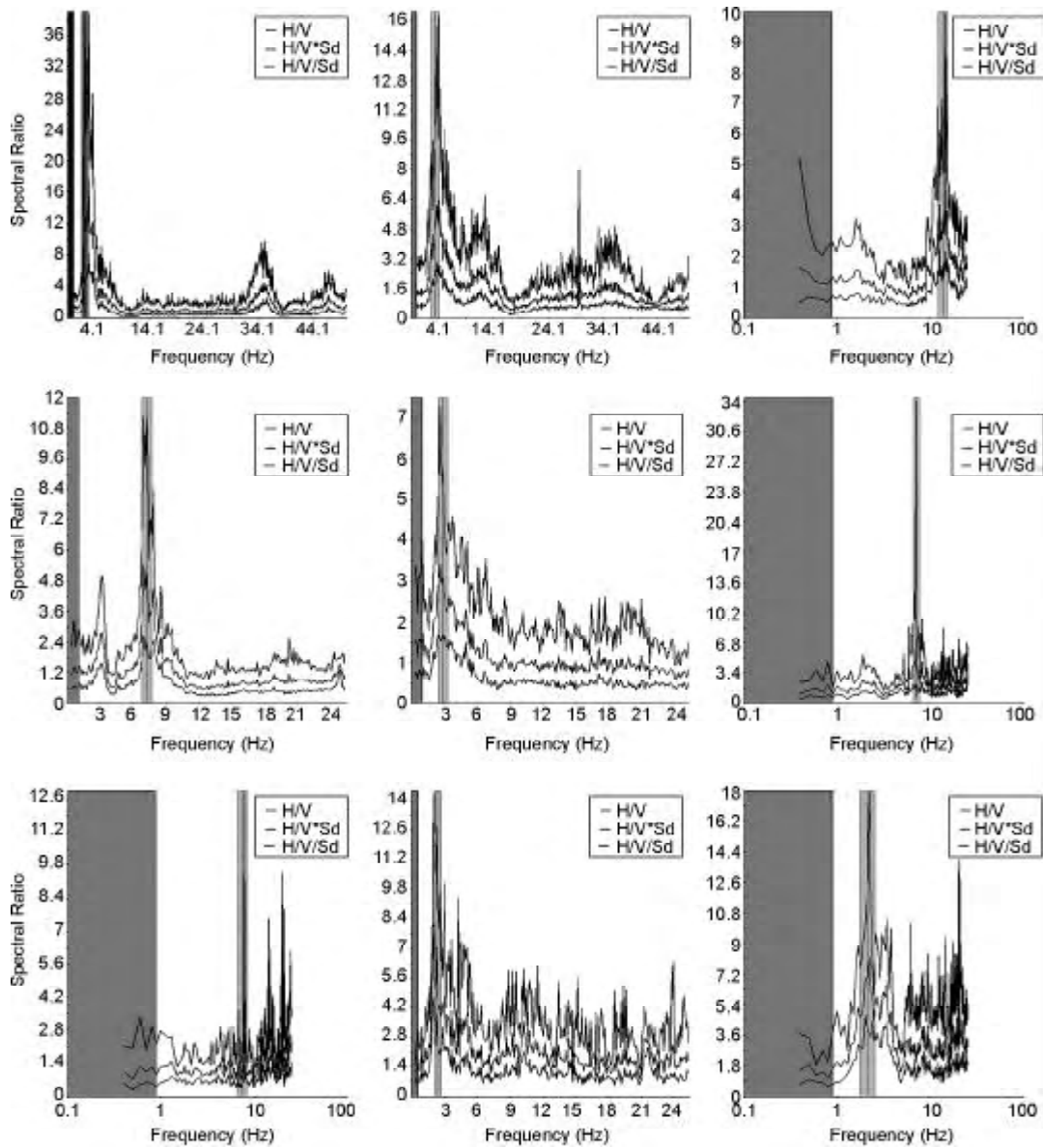


Figure 10. H/V spectra of microtremor.

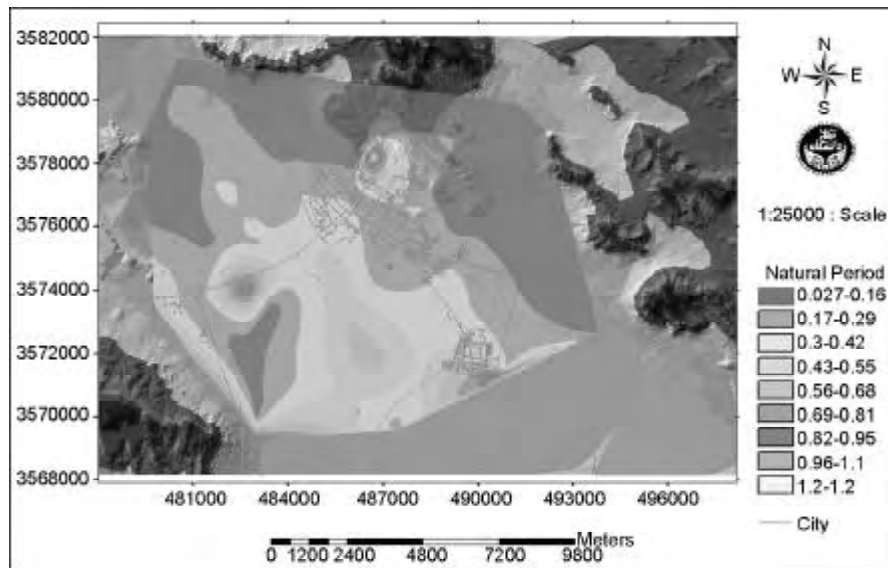


Figure 11. Natural period map.

Table 1. Location, frequency, period and amplification results.

| No | X | Y | Frequency | Period | Amplification |
|-----|--------|---------|-----------|--------|---------------|
| m1 | 487425 | 3576653 | 4.10 | 0.24 | 14 |
| m2 | 486250 | 3578133 | 43.10 | 0.02 | 20 |
| m3 | 486642 | 3578194 | 0.80 | 1.25 | 3 |
| m4 | 485333 | 3576225 | 3.00 | 0.33 | 20 |
| m5 | 490792 | 3571323 | 1.00 | 1.00 | 4 |
| m6 | 483814 | 3574626 | 2.50 | 0.40 | 5 |
| s1 | 484474 | 3579151 | 36.00 | 0.03 | 10 |
| s2 | 483742 | 3578660 | 9.00 | 0.11 | 5 |
| s3 | 484314 | 3577119 | 3.50 | 0.29 | 28 |
| s4 | 484599 | 3575579 | 3.00 | 0.33 | 38 |
| s5 | 486040 | 3577455 | 4.00 | 0.25 | 5 |
| s6 | 488052 | 3576498 | 3.00 | 0.33 | 9 |
| s8 | 487453 | 3578716 | 3.50 | 0.29 | 16 |
| s9 | 486829 | 3560581 | 14.00 | 0.07 | 10 |
| s10 | 487187 | 3574683 | 7.00 | 0.14 | 6 |
| s11 | 485153 | 3578534 | 12.00 | 0.08 | 4 |
| s12 | 489043 | 3574342 | 3.00 | 0.33 | 6 |
| s13 | 489359 | 3576097 | 13.00 | 0.08 | 8 |
| s14 | 491140 | 3579482 | 15.00 | 0.07 | 6 |
| s15 | 491323 | 3579882 | 23.00 | 0.04 | 10 |
| s16 | 489751 | 3576189 | 7.00 | 0.14 | 10 |
| s17 | 493854 | 3572644 | 7.00 | 0.14 | 12 |
| s18 | 492364 | 3574339 | 12.00 | 0.08 | 5 |
| s19 | 490923 | 3571569 | 4.00 | 0.25 | 10 |
| s20 | 480506 | 3581344 | 18.00 | 0.06 | 6 |
| p1 | 480242 | 3580728 | 13.00 | 0.08 | 7 |
| p2 | 480581 | 3579927 | 4.00 | 0.25 | 7 |
| p3 | 479534 | 3579252 | 24.10 | 0.04 | 7 |
| p4 | 479663 | 3578513 | 24.10 | 0.04 | 13 |
| p5 | 480185 | 3578019 | 19.00 | 0.05 | 4 |
| p6 | 480916 | 3577648 | 24.10 | 0.04 | 22 |
| p7 | 479555 | 3576912 | 24.10 | 0.04 | 15 |

| No | X | Y | Frequency | Period | Amplification |
|-------|--------|---------|-----------|--------|---------------|
| p8 | 481830 | 3577277 | 3.00 | 0.33 | 7 |
| p9 | 483634 | 3576873 | 5.50 | 0.18 | 6 |
| p10 | 481644 | 3575584 | 7.00 | 0.14 | 34 |
| p11 | 482899 | 3575736 | 3.00 | 0.33 | 24 |
| p12 | 482899 | 3575551 | 4.10 | 0.24 | 11 |
| p13 | 484364 | 3575702 | 3.00 | 0.33 | 13 |
| p14 | 479731 | 3573494 | 2.00 | 0.50 | 10 |
| p15 | 481092 | 3573706 | 7.00 | 0.14 | 9 |
| p16 | 482948 | 3569208 | 1.00 | 1.00 | 7 |
| p17 | 482995 | 3570008 | 8.00 | 0.13 | 13 |
| p18 | 482606 | 3572195 | 12.00 | 0.08 | 16 |
| p19 | 482661 | 3573950 | 1.00 | 1.00 | 8 |
| p20 | 483366 | 3573302 | 16.50 | 0.06 | 11 |
| p21 | 484780 | 3574347 | 2.50 | 0.40 | 15 |
| p22 | 484545 | 3574717 | 2.50 | 0.40 | 8 |
| p23 | 484781 | 3575240 | 2.50 | 0.40 | 15 |
| p24 | 485435 | 3574808 | 2.00 | 0.50 | 18 |
| p25 | 485981 | 3572990 | 1.80 | 0.56 | 8 |
| p26 | 486529 | 3571912 | 1.50 | 0.67 | 9 |
| p27 | 488098 | 3571448 | 2.50 | 0.40 | 18 |
| P30.1 | 482986 | 3580262 | 9.00 | 0.11 | 4 |
| P30.5 | 484135 | 3580173 | 23.00 | 0.04 | 8 |
| p28 | 487389 | 3569663 | 4.00 | 0.25 | 7 |
| p29 | 484970 | 3578657 | 22.00 | 0.05 | 5 |
| p30 | 492158 | 3579049 | 32.00 | 0.03 | 10 |
| p31 | 490301 | 3577542 | 15.00 | 0.07 | 7 |
| p32 | 489254 | 3576804 | 18.00 | 0.06 | 7 |
| p33 | 489071 | 3576805 | 20.00 | 0.05 | 19 |
| p34 | 492600 | 3575385 | 23.00 | 0.04 | 34 |
| p35 | 491399 | 3577264 | 20.00 | 0.05 | 6 |
| p36 | 487494 | 3569540 | 3.80 | 0.26 | 24 |
| p37 | 491370 | 3574216 | 7.00 | 0.14 | 5 |

Natural periods are very high in Kiyan city and the center of the plain due to the soil thickness. This case study indicates that the natural frequency is strongly in accordance with the bedrock level change and soil thickness. The represented zonation maps can be used as the basic maps in the constructions. Therefore, according to $T = \frac{N}{10}$ Equation (N : number of floors, T : natural period of buildings), the optimal number of floors can be attained for preventing the resonance phenomena in the new urban areas. For example, regarding the mentioned classification, 1 story-buildings are exposed to the resonance hazard with natural period of 0.1s and 12 story-buildings with 1.2s. The amplification factor and natural period are calculated and zoned into 9 classes. As it is seen in Figure (12), the amplification factor follows no

specific trend and depends only on the frequencies. Trend increasing can be observed in the city center in the middle of the field and eastern-western foot of the mountains.

9. Velocity Measurement

To figure out the shear wave velocity, refraction method is applied within the limits of the city. Seismic refraction method is appropriate for general site study regarding subsurface conditions [10]. In order to increase the wave penetration depth for each profile (the mentioned 20 stations), P body waves and shear-waves are appraised using 9-11 and 6-8 seismic sources, respectively. The calculation and their relevant formulas, regarding the profiles of soil and rock layers, were mentioned earlier including the

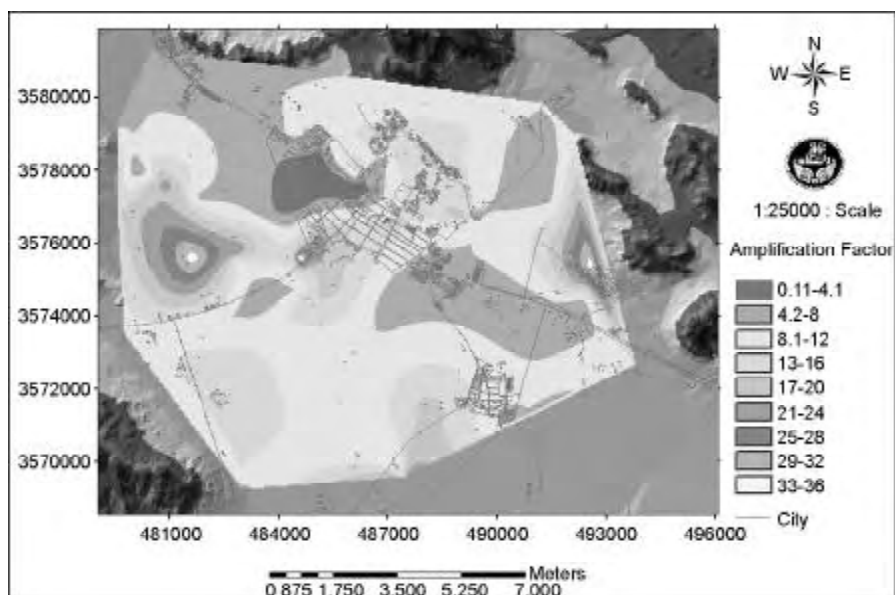


Figure 12. Amplification factor map.

classification of soil deposited on rock and the depth less than 30m. The results are represented in Table (2). Shear-wave velocity is classified in 6 levels with the minimum of 246m/s and maximum of 1150m/s. Shear-wave velocity shows an increasing trend toward northeast illustrated in Figure (13).

The accuracy of microtremor measurements is qualified using Dobri Eq. $T = \frac{4H}{VS}$ for stations with certain thicknesses and shear-wave velocities. Shahrekord site is classified according to Zare et al [11] using shear-waves and microtremors data, see

Figure (14). In brief, over 30m soil depth, the sites are categorized as:

- The 1st site category: Corresponds to rock and hard alluvium with average VS of >700m/s and site amplification (SAM) of >15Hz;
- The 2nd site category: related to the alluvium sites (thin soft alluviums) with 500 < VS < 700, and 5 < SAM < 15Hz;
- The 3rd site category: soft gravel and sandy sites with 300 < VS < 500 and 2 < SAM < 5Hz;
- The 4th site category: related to soft soil sites

Table 2. Shear wave velocity location in different layers.

| Longitude | Latitude | $\overline{V_{s30}}$ | First Thickness Layer | Second Thickness Layer | Third Thickness Layer | First Velocity Layer | Second Velocity Layer | Third Velocity Layer |
|-----------|----------|----------------------|-----------------------|------------------------|-----------------------|----------------------|-----------------------|----------------------|
| 483708 | 3579934 | 716 | 12.7 | 17.3 | - | 565 | 890 | - |
| 483687 | 3578399 | 720 | 15 | 15 | - | 580 | 950 | - |
| 484097 | 3577274 | 266 | 23.4 | 6.6 | - | 235 | 495 | - |
| 484429 | 3575800 | 290 | 23.7 | 6.3 | - | 270 | 400 | - |
| 486062 | 3577220 | 845 | 8.9 | 21.1 | - | 570 | 1060 | - |
| 488070 | 3576617 | 540 | 12.4 | 17.6 | - | 330 | 980 | - |
| 488694 | 3577757 | 632 | 6.5 | 4.4 | 19.1 | 250 | 725 | 1240 |
| 487812 | 3578757 | 1152 | 11.9 | 18.1 | - | 685 | 2090 | - |
| 486704 | 3579108 | 822 | 11.8 | 18.2 | - | 465 | 1635 | - |
| 486648 | 3575107 | 244 | 9.3 | 8.6 | 12.1 | 160 | 275 | 360 |
| 485474 | 3578393 | 874 | 25.4 | 4.6 | - | 805 | 1650 | - |
| 489044 | 3574290 | 341 | 23.2 | 6.8 | - | 285 | 1020 | - |
| 489482 | 3575636 | 387 | 9.2 | 20.8 | - | 165 | 960 | - |
| 490929 | 3578943 | 681 | 12.8 | 17.2 | - | 460 | 1060 | - |
| 492258 | 3579931 | 898 | 4.6 | 25.4 | - | 475 | 1070 | - |
| 490585 | 3576686 | 600 | 21 | 3.3 | 5.7 | 495 | 865 | 1520 |
| 493975 | 3572622 | 375 | 8.1 | 6.8 | 15.1 | 180 | 345 | 990 |
| 492127 | 3574897 | 503 | 18 | 9.5 | 2.5 | 370 | 995 | 1790 |
| 491147 | 3573083 | 324 | 10.6 | 11.4 | 8 | 215 | 345 | 790 |
| 480881 | 3580818 | 313 | 10.8 | 7.1 | 12.1 | 190 | 405 | 560 |

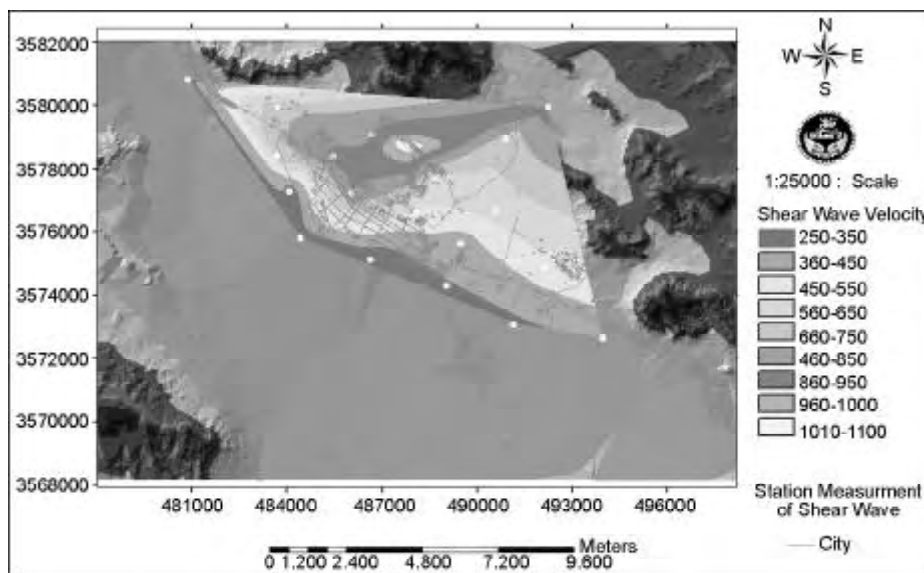


Figure 13. Shear wave velocity map with increasing trend towards northeast.

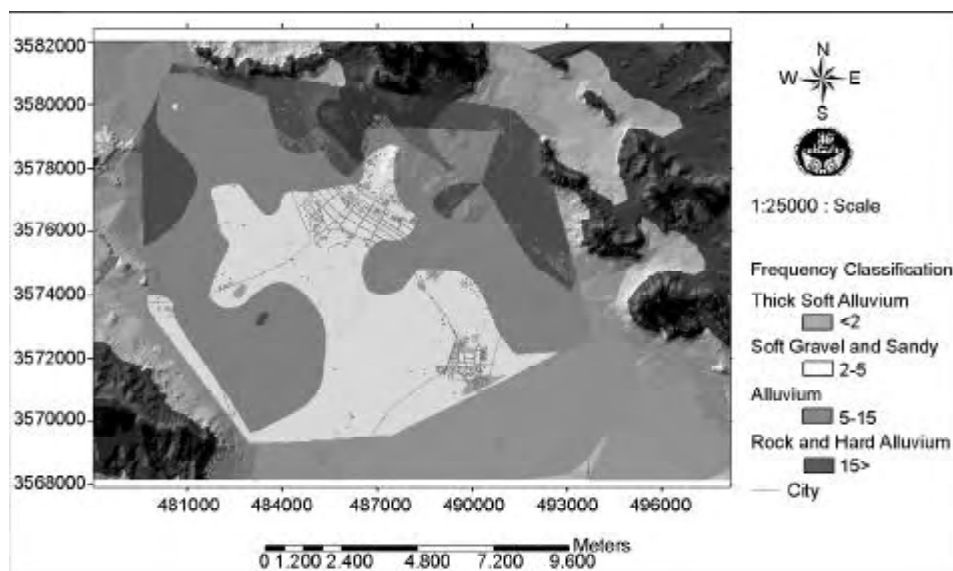


Figure 14. Site classification.

(thick soft alluviums) with $V_S < 300m/s$ and $SAM < 2Hz$, Table (3) [4, 11].

Therefore, the study area is divided into 4 structural ranges. The shear wave velocities where overlap the microtremor recording, are properly in accordance with natural frequencies obtained by microtremor, as expected. Therefore, the shear wave velocity increases approaching northeast, where the natural frequency is higher.

Consequently, the overlaying of maps and DEM show that the mountain and hard land are near. This process is true in the south-west as well. The obtained map can be used in calculating the seismic spectral response in civil engineering. The accelerograms of

other places of similar soil can be used for the study area with soil kind sampling.

10. Conclusion

Using microtremor and shear-wave velocity are widely promoted in studying site effects and seismic microzonation. Today the role of site effects in the size of earthquake damage is completely clear. Therefore, in this study, the site effects are analyzed by microtremor and shear-wave velocity using geotechnical data. The results of such studies lead in making natural period, amplification factor, soil classification and geological engineering maps.

The structural situation of a zone can properly

Table 3. Zare et al [11].

| Frequency Band of the Amplification | Shear-Wave Velocity over the Top 30m | Group |
|-------------------------------------|--------------------------------------|------------------------|
| Rhv(Amp) > 15HZ | 700 < Vs30 | Rock and Hard Alluvial |
| 5 < Rhv(Amp) < 15HZ | 500 < Vs30 < 700 | Alluvium |
| 2 < Rhv(Amp) < 5Hz | 300 < Vs30 < 500 | Soft Gravel and Sandy |
| Rhv(Amp) < 2Hz | Vs30 < 300 | Thick Soft Alluvium |

be estimated by applying three kinds of data. The exactness of the experiments is related to how the data are measured. The more precisely the data are collected, the more possibilities in accessing the layer under surface conditions. In this study first, the ground deformation is investigated and the fundamental maps such as slope, slope orientation, alluvium depth, raining amount, velocity and underground water level are prepared. Then the rockfall and liquefaction phenomena are studied. A problem in studying urban zones is that the ground is covered by roads and constructions. Therefore, microtremors are the cheapest and most applicable means of studying such zones. In this research the microtremors are studied at 65 stations. Studying the microtremors leads to preparing natural period maps and site amplification factor. Urban structures can be categorized, regarding soil types, using shear wave velocity and microtremors, which has been done here according to Zare et al [11].

Therefore, in this study Shahrekord is zoned by different methods and views. Each method leads to a series of information layers which are the basis of decision in urban developing or reinforcement against natural disasters.

Concerning the number of stories and importance of the buildings, they should be constructed in the areas of the least site natural period. Here it can be concluded that the Northeast-Southwest is the best direction for new construction in urban areas.

It should be considered that the rockfall and landslide hazard increase near the mountain and foot of mountain. Finally the places, located in the best area regarding geological engineering and seismicity, should be selected.

Acknowledgment

The author would like to extend his gratitude to Dr. M. Zare, Associate Professor of *IIEES*, for his constructive comments on this research. Ms. Zh. Torabi Jahromi is also appreciated for her cooperation in editing the paper.

References

1. Mojarab, M., Memarian, H., Zare, M., and Roozkhah, P. (2007). "A GIS Based Landslide Potential Zonation Based on Earthquake Hazard", Map Asia, Malaysia, Full Paper on CD Proceedings.
2. Mojarab, M., Memarian, H., Zare, M., and Roozkhah, P. (2007). "Study of Site Effect Using The Microtremors", *Second Disaster Management Conference*, Full Paper on CD Proceedings.
3. Mojarab, M., Memarian, H., Zare, M., and Roozkhah, P. (2006). "Geological Engineering Zonation Using GIS", *First Disaster Management Conference*, **3**, 229-238.
4. Bard, P.-Y., Zare, M., and Ghafory-Ashtiany, M. (1998). "The Iranian Accelerometric Data Bank, A Revision and Data Correction", *Journal of Seismology and Earthquake Engineering*, **1** (1), 1-22.
5. Nakamura, Y.A. (1989). "Method for Dynamic Characteristics Estimation of Subsurface Using Microtremor on the Ground Surface", Quarterly Report of RTRI, Railway Technical Research (RTRI), **30**(1), 25-33.
6. Nakamura, Y.A. (1971). "Seismic Vulnerability Indices for Ground and Structures Using Microtremor", *World Congress on Railway Research in Florence, Italy*.
7. Nogoshi, M. and Igarashi, T. (1989). "On the Amplitude Characteristics of Microtremor, Part 2", (In Japanese with English Abstract), *Journal Seism. Soc. Japan*, **24**, 26-40.
8. Nakamura, Y. and Samizo, M. (1989). "Site Effect Evaluation of Surface Ground Using Strong Motion Records (in Japanese)", *Proc. 20th JSCE Earthquake Eng. Symposium*, 133-136.

9. Bard, P.Y. (1998). "Microtremor Measurements: A Tool for Site Effect Estimation?", *Proc. of 2nd International Symposium on the Effect of Surface Geology on Seismic Motion*, Yokohama, Japan.
10. Dobry, R. (2000). "New Site Coefficients and Site Classification System Used in Recent Building Seismic Code Provisions", *Earthquake Spectra*, **16**(1).
11. Zare, M., Bard, P.-Y., and Ghafory-Ashtiany, M. (1999). "Site Characterizations for the Iranian Strong Motion Network", *Soil Dyn. Earthquake Eng.*, **18**, 101-123.
12. Chavez, F.G., Garcia, F.G., and Bard, P.Y. (1990). "An Experimental Study of Effects Near Theassaloniki", *Bull. Seism. Soc. Am.*, **80**, 847-806.
13. Field, E.H. and Jacob, K.H. (1990). "Using Microtremor to Asses Potential Earthquake Site Response", *Bull. Seism. Soc. Am.*, **80**, 1456-1480.
14. Ghayamghamian, M.R. and Kawakami, H. (1997). "Semental Cross-Spectrum in Microtremor Spectral Ratio Analysis", *7th Conference on Structural Safety and Reliability*, Kyoto, 1487-1494.
15. Kagami, H. and Okada, S. (1986). "Observation of 1 to 5 Second Microtermors and Their Application to Earthquake Engineering", *Bull. Seism. Soc. Am.*, 1801-1812.
16. Lermo, J., Chavez, F.G., and Garcia, F.J. (1993). "Site Effect Evaluation Using Spectral Ratios with Only One Station", *Bull. of Seism. Soc. An.*, **183**, 1574-1594.
17. Singh, S.K. (1993). "A Site Effect Study in Acapulco Guerrero, Mexico, Comparison of Results of Strong Motions and Microtermor Data", *Bull. Seism. Soc. Am.*, **82**, 642-659.
18. Yamanaka, H. (1993). "Continuous Measurement of Microtermors on Sediments and Basement in Los Angeles", *Bull. Seism. Soc. Am.*, 1595-1604.
19. Yamazaki, F. and Katayama, I. (1992). "Soil Amplification Based on Seismometer Array and Microtermor Observations in Chiba, Japan", *Earthquake Engineering Soil. Dyn.*, **21**, 95-108.
20. Mehraein, L. and Tatar, M. (2006). "Site Effect Study in Southwest of Tehran Using Microtremor Measurements", *Geosciences Journal*, **15**(59), 24-37.
21. Huang, H.C. and Teng, T.L. (1999). "An Evaluation on H/V Ratio Vs. Spectral Ratio for Site Response Estimation Using the 1994 Northridge Earthquake Sequence", *Pure and Applied Geophysics*, **156**, 631-649.